Orbital order parameter in $La_{0.95}Sr_{0.05}MnO_3$ probed by electron spin resonance

J. Deisenhofer,[1] B. I. Kochelaev,[2] E. Shilova,[2] A. M. Balbashov,[3] A. Loidl,[1] and H.-A. Krug von Nidda[1]
[1]*Experimentalphysik V, Center for Electronic Correlations and Magnetism, Institute for Physics, Augsburg University, D-86135 Augsburg, Germany*
[2]*Kazan State University, 420008 Kazan, Russia*
[1]*Moscow Power Engineering Institute, 105835 Moscow, Russia*
(Received 29 September 2003; published 24 December 2003)

The temperature dependence of the electron-spin resonance in $La_{0.95}Sr_{0.05}MnO_3$ has been investigated and analyzed in the paramagnetic regime across the orbital ordering transition. From the temperature dependence and the anisotropy of linewidth and g value the orbital order can be unambiguously determined via the mixing angle of the wave functions of the e_g doublet. The linewidth shows a similar evolution with temperature as resonant x-ray scattering results.

DOI: 10.1103/PhysRevB.68.214427 PACS number(s): 76.30.−v, 75.30.Et

In transition-metal oxides the orbital degrees of freedom play an important role for the electric and magnetic properties.[1] Their coupling to spin, charge, and lattice is responsible for the occurrence of a variety of complex electronic ground states. Orbital order (OO) can be derived via the Jahn-Teller (JT) effect[2] or via superexchange (SE) between degenerate orbitals under the control of strong Hund's-rule coupling.[3] Strong correlations exist between spin and orbital order and between OO and lattice distortions, but of course a one-to-one correspondence cannot be expected. While spin and lattice order can easily be detected experimentally, this is not true for OO and so far the OO parameter remains hidden. In recent years resonant x-ray scattering (RXS) has been used to derive information on the OO parameter,[4] but there is an ongoing dispute, whether RXS probes the JT distortion or the orbital charge distribution.[5,6] Indirectly, OO can also be derived from diffraction experiments via lattice distortions and bond lengths.[7–10] In this work we demonstrate that electron-spin resonance (ESR) can be used to detect OO and to monitor the evolution of the OO parameter. Probing the spin of the partially filled d shell of the Mn^{3+} ions by ESR, the anisotropy and temperature dependence of g value and linewidth ΔH provide clear information on OO via spin-orbit (SO) coupling.

The power of ESR to gain insight into OO will be demonstrated on A-type antiferromagnetic (AFM) $LaMnO_3$ ($T_N = 140$ K), the parent compound of the magnetoresistance manganites and a paradigm for a cooperative JT effect that suggests a $d_{3x^2-r^2}/d_{3y^2-r^2}$-type OO below $T_{JT}=750$ K.[11] However, it has been shown that SE interactions play an important role, too.[12] Several recent studies exhibit clear anomalies of the ESR parameters at the JT transition in both doped and pure $LaMnO_3$.[13–16] The orbitally ordered O' phase is characterized by an anisotropy of ΔH,[16,17] which for polycrystalline samples reduces to a broad maximum in $\Delta H(T)$.[14,15] Previously, the angular dependences of ΔH and the resonance field H_{res} had been analyzed for 200 K and 300 K in high-temperature approximation, allowing to estimate the Dzyaloshinsky-Moriya (DM) interaction and the strength of the zero-field splitting (ZFS) parameters.[18] At X-band frequencies (9 GHz) ΔH was of the same order of magnitude as H_{res} and due to the overlap with the resonance at $-H_{res}$ and their mutual coupling via the nondiagonal elements of the dynamic susceptibility[19] the values for H_{res} contained a rather large uncertainty. To avoid these problems we performed new experiments at Q-band frequencies (34 GHz), which allowed a better determination of H_{res}.

The scope of the present paper is the comprehensive analysis of the temperature dependence and anisotropy of ΔH and the g value of the ESR signal in $La_{0.95}Sr_{0.05}MnO_3$. We chose this concentration for the present study as an untwinned single crystal was available and $T_{JT}\sim 605$ K is accessible to our experimental setup.[20,21]

ESR measurements were performed with a Bruker ELEXSYS E500 CW spectrometer at X- ($\nu\approx 9.4$ GHz, $4.2\ \text{K}\leqslant T \leqslant 670$ K) and Q-band frequencies ($\nu\approx 34$ GHz, $4.2\ \text{K}\leqslant T \leqslant 290$ K), using a continuous gas-flow cryostat for He (Oxford). The oriented sample was mounted in a quartz tube with paraffin. A goniometer allowed the rotation of the sample around an axis perpendicular to the static magnetic field $\vec{H}_{ext}$.

Figure 1(a) shows ΔH for X-band frequency and Fig. 2 shows ΔH (inset) and the effective g value $g_{eff} = h\nu/(\mu_B H_{res})$ determined from H_{res} for Q-band frequency. The observed linewidths at both frequencies nicely coincide. Only near the minimum below 200 K the absolute values are slightly enhanced at 34 GHz as compared to 9 GHz. While the g values obtained at X-band frequency bear a rather large uncertainty,[16,18] at Q-band frequency the g values show a regular temperature dependence, approaching a constant high-temperature value and increasing for $T\rightarrow T_N$. First, we determined the ZFS parameters D and E from the temperature dependence of H_{res} at Q-band frequency. Using the general formula for the resonance shift due to crystal-field (CF) effects[18,22] and accounting only for the rotation (angle γ) of the MnO_6 octahedra in the ac plane (axis notation such as in Ref. 23), we obtained the following expressions for the effective g values for $\vec{H}_{ext}$ applied along one of the crystallographic axes

$$\frac{g_{a,c}^{eff}(T)}{g_{a,c}} \approx 1 + \frac{D}{T-T_{CW}}[(3\zeta-1) \pm 3(1+\zeta)\sin(2\gamma)], \quad (1)$$

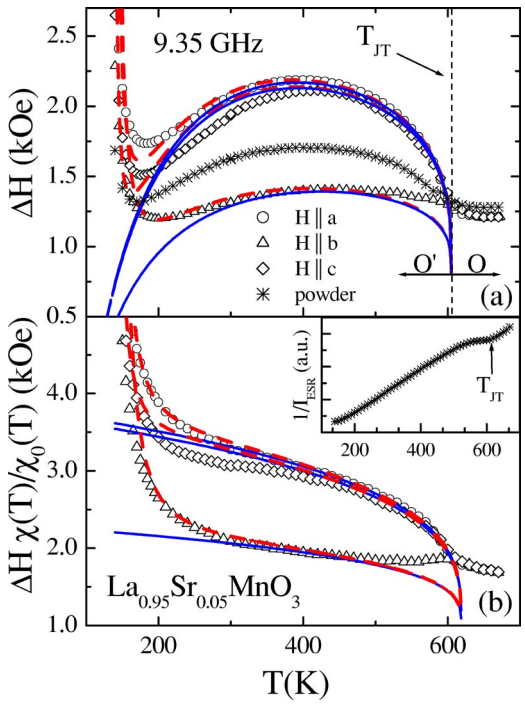

FIG. 1. Temperature dependences of (a) $\Delta H(T)$ and (b) $\Delta H \cdot \chi(T)/\chi_0(T)$ at 9.35 GHz for $\vec{H}_{\rm ext}$ parallel to the crystallographic axes. Solid and dashed lines represent fits using Eq. (3) as described in the text. Inset: temperature dependence of the inverse ESR intensity of a polycrystalline sample.

$$\frac{g_b^{\rm eff}(T)}{g_b} \approx 1 - \frac{2D}{T - T_{\rm CW}}(3\zeta - 1), \tag{2}$$

with the Curie-Weiss (CW) temperature $T_{\rm CW}$ and $\zeta = E/D$. All terms of second and higher order in $D/(T - T_{\rm CW})$ were neglected. The temperature dependence of the effective g values is, hence, given by the CW law of the magnetic susceptibility. Excluding the critical regime on approaching magnetic order below 170 K, the data are well described by this approach (solid lines in Fig. 2), where $T_{\rm CW}$ was kept

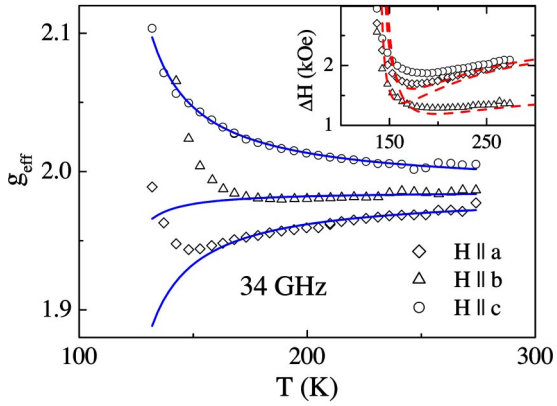

FIG. 2. Temperature dependence of the effective g value $g_{\rm eff}(T)$ and $\Delta H(T)$ (inset) at 34 GHz for $\vec{H}_{\rm ext}$ parallel to the crystallographic axes. The solid lines represent fits using Eqs. (1) and (2) for $g_{\rm eff}$, the dashed lines for ΔH are the same as in Fig. 1(a).

fixed at 111 K.[16] The rotation angle was chosen as $\gamma = 13°$ as observed in pure $LaMnO_3$.[7,23] Then all data can be consistently described by $D = 0.60(2)$ K, the E/D-ratio $\zeta = 0.37(1)$, and the g values $g_a = 1.988(1)$, $g_b = 1.986(1)$, and $g_c = 1.984(1)$. From these crystallographic g values, the local g values of Mn^{3+} can be calculated as $g_z = 1.977$, g_y $(= g_b) = 1.986$, and $g_x = 1.995$, typical for ions with less than half-filled $3d$ shell with the longest and shortest Mn-O bond along the local z and x direction, respectively.[24]

The main result of this evaluation is the E/D ratio, which we improved in comparison to our previous estimate[18] by the Q-band experiment. For $\vec{H}_{\rm ext}$ applied along the b axis the data are nearly T independent, whereas they clearly exhibit the CW behavior for the other orientations. Regarding the equation for g_b, this is only possible, if the factor $(3\zeta - 1)$ is close to zero and hence $\zeta \approx 1/3$. This result is independent of the value of the rotation angle γ. Only the absolute value of D directly depends on the choice of γ, which accounts for the splitting of the resonance fields between a and c direction.

With the obtained E/D ratio we now focus on the linewidth data. A detailed derivation of the CF contributions to ΔH in the cooperatively JT distorted perovskite structure accounting for the mutual rotations of the MnO_6 octahedra is presented in Ref. 25. This theoretical approach can be summarized in the formula

$$\Delta H^{(\vartheta,\varphi)}(T) = \frac{\chi_0(T)}{\chi(T)}\left\{\Gamma_{\rm DM} + t^{2\beta}\left[\Gamma_{\rm CF} f_{\rm reg}^{(\vartheta,\varphi)} + \Gamma_{\rm CFD}\left(\frac{T_{\rm N}}{6(T - T_{\rm N})}\right)^{\alpha} f_{\rm div}^{(\vartheta,\varphi)}\right]\right\}, \tag{3}$$

with the free Curie susceptibility $\chi_0 \propto T^{-1}$, the static susceptibility $\chi(T)$, and $t = 1 - T/T_{\rm JT}$. The first term describes the contribution $\Gamma_{\rm DM}$ of the DM interaction as introduced by Huber *et al.*[13] This contribution is expected to survive the JT transition and hence to determine the line broadening also at $T > T_{\rm JT}$. The second and third term, $\Gamma_{\rm CF}$ and $\Gamma_{\rm CFD}$, represent the regular and divergent CF contributions, respectively. Only the latter diverges for $T \to T_{\rm N}$ with an exponent α, whereas both terms decrease for $T \to T_{\rm JT}$ with a critical exponent 2β, with β being the critical exponent of the ZFS parameters D and E. The angular factors $f_{\rm reg}^{(\vartheta,\varphi)}$ and $f_{\rm div}^{(\vartheta,\varphi)}$ read

$$f_{\rm reg}^{(\vartheta,\varphi)} = f_{\rm div} + (1 + \zeta)^2\left(1 + \tfrac{3}{2}\sin^2\vartheta\right),$$

$$f_{\rm div}^{(\vartheta,\varphi)} = \tfrac{1}{2}[1 - 3\zeta + 2\gamma(1 + \zeta)]^2(1 - \sin^2\vartheta\,\sin^2\varphi) + \tfrac{1}{2}[1 - 3\zeta - 2\gamma(1 + \zeta)]^2(1 - \sin^2\vartheta\,\cos^2\varphi),$$

where ϑ and φ are the polar and azimuthal angles between $\vec{H}_{\rm ext}$ and the crystallographic b and c axes, respectively. An analogous calculation to the one presented in Ref. 25 showed that the DM interaction does not exhibit any critical behavior at $T_{\rm N}$. To minimize the number of fit parameters, we neglected here any angular dependence of the DM contribution. In first approximation this is justified by the observation that above $T_{\rm JT}$ the linewidth is isotropic. However, generally an

anisotropy of the DM contribution can arise in the orbitally ordered state.[18] But it consists itself at least in two contributions from different Mn-O-Mn bond geometries, and its transformation to an isotropic behavior on approaching T_{JT} needs further theoretical considerations. The susceptibility $\chi(T)$ can be approximated by a CW law in case of T independent exchange constants. At T_{JT}, however, a kink shows up in $\chi(T)$ resulting in a higher CW temperature obtained from data above the transition,[20] a fact that demands caution when assuming a CW law throughout the whole O' phase, as the fitting parameters, especially β, could be influenced by changes in the exchange constants. To check the sensitivity of the fit results to the susceptibility anomaly at T_{JT}, we evaluated the linewidth data both with a simple CW term [Fig. 1(a)] and using the real susceptibility [Fig. 1(b)]. In the latter case we transformed the linewidth data into $\Delta H \cdot \chi(T)/\chi_0(T)$ [see Eq. (4)]. The spin susceptibility was determined by the ESR intensity I_{ESR} of a powder sample, in order to avoid the influence of the skin effect.[16] To illustrate the coincidence of the JT transition of both the single crystal and the polycrystalline material, the temperature dependence of $1/I_{ESR}$ is shown in the inset of Fig. 1(b) and the corresponding linewidth is included in Fig. 1(a). It turned out that the fit results are stable with respect to these two procedures. Only the transition temperature $T_{JT}=618$ K is slightly higher than 605 K when using the experimental susceptibility instead of a pure CW behavior. But both values remain within the experimental uncertainty of $\Delta T_{JT}=\pm 10$ K for the transition temperatures for both single crystal and powder sample.

In the minimal model we omitted the divergent CF contribution ($\Gamma_{CFD}=0$), kept the CW temperature fixed at $T_{CW}=111$ K, and the rotation angle in the ac plane was set to $\gamma=13°$. In addition, the parameter $\zeta=0.37$ was taken from the evaluation of the g values. The JT temperature was allowed to vary between 600 K and 620 K. So only three fit parameters remain, the regular part of the CF contribution Γ_{CF}, its critical exponent β at the JT transition, and the DM contribution Γ_{DM}. A simultaneous fit (Fig. 1: solid lines) of $\Delta H(T)$ is satisfactorily performed above 200 K with $\Gamma_{DM}=1.0(1)$ kOe, $\Gamma_{CF}=0.57(2)$ kOe, and $\beta=0.16(1)$.

Finally, we added the effect of the divergent CF contribution, which allows us to increase the splitting between ΔH_a and ΔH_c to lower temperatures, as observed in the experiment. As shown in Fig. 1 (dashed lines) a qualitative description was obtained by fitting the X-band data with $\Gamma_{CFD}=10$ kOe and $\alpha=1.8$ with fixed $T_N=135$ K. To show the good agreement of the X- and Q-band data, we display the same fit curves in the inset of Fig. 2. Theoretically, a smaller exponent $\alpha_{theo}=0.75$ is expected, but a pure power law holds only for temperatures close to T_N.[25]

The DM contribution $\Gamma_{DM}=1.0$ kOe determined in the O' phase is lower than the one expected from $\Delta H \approx 1.4$ kOe in the O' phase. This discrepancy can be explained by contributions of the CF due to the dynamic JT effect present in the O' phase.[26] Comparison with the regular CF contribution $\Gamma_{CF}=0.57$ kOe allows us to estimate the averaged value D_{DM} of the DM interaction as defined in Ref. 13. The ratio of the linewidth contributions equals the ratio of the respective second moments approximated by $10(D_{DM}/D)^2 \approx \Gamma_{DM}/\Gamma_{CF}$.[13] With $D=0.6$ K one obtains $D_{DM} \approx 0.25$ K. These values are free from the uncertainty in the estimation of the exchange frequency in the exchange-narrowed linewidth,[25] because we used the g values to determine the absolute values. Though being smaller than earlier estimates for polycrystalline $LaMnO_3$ their relative strength is in good agreement with previous results.[13,14]

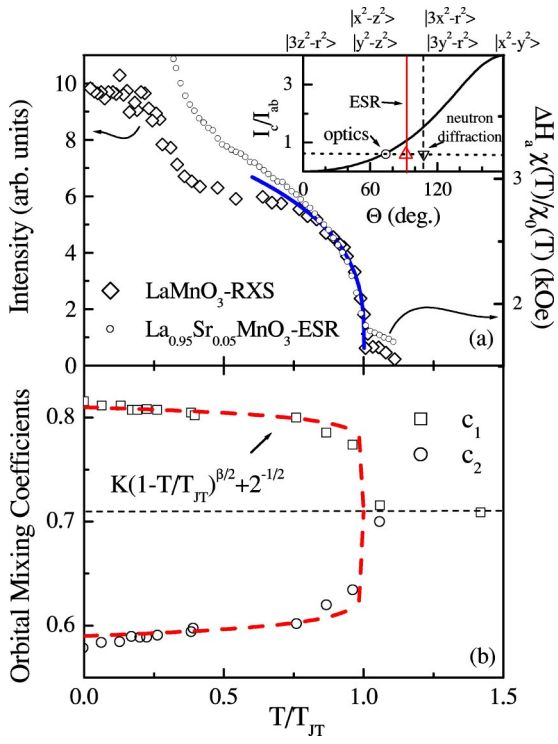

FIG. 3. Temperature dependence of (a) the reduced ESR linewidth in $La_{0.95}Sr_{0.05}MnO_3$ compared to the RXS intensity of $LaMnO_3$ taken from Ref. 4. The solid line is a fit of the RXS intensity as described in the text. Inset: Θ dependence of the normalized optical spectral weight I_c/I_{ab} following Ref. 28 (solid line) with the experimentally derived Θ values; (b) temperature dependence of c_1 and c_2 determined by neutron diffraction taken from Ref. 7. The dashed lines were obtained using $K(1-T/T_{JT})^{0.08}+2^{-1/2}$.

After having extracted the ZFS parameters we will now discuss the consequences for OO in $LaMnO_3$: In Fig. 3(a) the transformed ESR linewidth $\Delta H_a \cdot \chi(T)/\chi_0(T)$ (for $\vec{H}_{ext} \| a$), which bears the critical behavior on approaching T_{JT} [see Eq. (4)], and the RXS intensity obtained by Murakami *et al.*[4] for $LaMnO_3$ are shown to visualize the similarity of the two quantities on approaching both T_N and T_{JT}. It has been pointed out that the RXS intensity close to T_{JT} is $\propto(1-T/T_{JT})^{2\beta}$,[6] where β denotes the critical exponent of the OO parameter given by the pseudo spin $\vec{T}=1/2(\sin\Theta,0,\cos\Theta)$.[6,27] The angle $\Theta=2\arctan(c_2/c_1)$ is a measure of the mixing of the wave functions of the e_g doublet in the ground state

$$\psi_g = c_1|3z^2-r^2\rangle + c_2|x^2-y^2\rangle. \quad (4)$$

To compare the results of RXS and ESR we fitted the RXS data in the vicinity of the JT transition ($650\ \mathrm{K} \leqslant T \leqslant T_{\mathrm{JT}} = 780\ \mathrm{K}$) with such a critical behavior [solid line in Fig. 3(a)] and obtained an exponent $\beta = 0.16(1)$ in agreement with the ESR linewidth. Considering that the ZFS parameters can be denoted as

$$D = -3(\rho + \lambda^2/\Delta)\cos\Theta, \tag{5}$$

$$E = -\sqrt{3}(\rho + \lambda^2/\Delta)\sin\Theta, \tag{6}$$

with the spin-spin coupling ρ, the SO coupling λ and the $t_{2g}-e_g$ splitting energy Δ,[24] it is easy to identify the relation with the OO parameter $\vec{T}$. Despite the lack of data in the critical regime, Fig. 3(b) shows the orbital mixing coefficients c_1 and c_2 determined from a neutron-diffraction (ND) study by Rodriguez-Carjaval *et al.*[7] The dashed lines were obtained by using

$$K(1 - T/T_{\mathrm{JT}})^{\beta/2} + 2^{-1/2}, \tag{7}$$

with $T_{\mathrm{JT}} = 750$ K and a critical exponent $\beta/2 = 0.08$ provided by $D \propto (c_1^2 - c_2^2)$ and $E \propto c_1 c_2$. With $K_1 = 0.10$ and $K_2 = -0.12$ the data for c_1 and c_2 can be well described throughout the JT distorted phase. However, attempting to describe the three data points in the critical regime rather suggests $\beta \sim 0.3$. Only a detailed structural study in the critical regime will allow a direct confirmation of the critical exponent for c_1 and c_2, but $\beta = 0.16$ as determined from ESR and RXS yields a reasonable description.

The main aim of this study is to estimate the angle $\Theta = \sqrt{3}\arctan(E/D)$ and to determine the type of OO by using the obtained value $E/D = 0.37(1)$, which after taking into account the transformation to a local coordinate system[25] results in $\Theta_{\mathrm{ESR}} \sim 92°$. Another estimate has been obtained from neutron diffraction via the orbital mixing coefficients at room temperature $c_1 \approx 0.8$ and $c_2 \approx 0.6$ resulting in $\Theta_{\mathrm{ND}} = 106°$.[7] This discrepancy cannot be easily explained. However, Tobe *et al.* tried to explain the anisotropy of the optical conductivity in $LaMnO_3$ on the basis of a *p-d* transition model by using the ratio

$$I_c/I_{ab} = 2(1 - \cos\Theta)/(2 + \cos\Theta) \tag{8}$$

between the optical spectral weight with the polarization within the ferromagnetic (FM) plane (there ab) and along the AFM axis (there c).[28] Their simple model [see inset of Fig. 3(a)] suggests a value $\Theta \sim 74°$ to describe the experimental value of $I_c/I_{ab} = 0.6$ at 10 K in the AFM regime. Theoretically, only a slight decrease of Θ below T_{N} is expected[12,29] and therefore $\Theta_{\mathrm{ESR}} \sim 92°$ yields a better description of the anisotropic properties of $LaMnO_3$ in the orbitally ordered state above T_{N} than $\Theta_{\mathrm{ND}} \sim 106°$. Alejandro *et al.* derived a similar E/D value from ESR data in $La_{7/8}Sr_{1/8}MnO_3$ in agreement with our result.[17] To the best of our knowledge no Θ estimate has been obtained by RXS and it is worthwhile to note that the RXS intensity becomes maximal for $\Theta = \pi/2$,[6] the value obtained by ESR. Following Maezono and coworkers $\Theta = \pi/2$ characterizes OO stabilized by the SE processes in the FM bonds and the electron-phonon coupling is small compared to the bandwidth.[27] Recent calculations by Sikora and Oleś suggest $\Theta = \pi/2$ at $T = T_{\mathrm{N}}$ and $\Theta = 83°$ at $T = 0$, in order to explain both the anisotropic exchange constants of $LaMnO_3$ and the high JT transition temperature.[29] These findings are in accordance with our experimentally derived value for the orbital ordering.

In summary, we were able to determine unambiguously the type of orbital ordering in paramagnetic $La_{0.95}Sr_{0.05}MnO_3$ by a consistent description of the temperature dependences of the effective g factor and the ESR linewidth. The evolution of the OO parameter monitored by the RXS intensity shows an intriguing similarity to the ESR linewidth. The derived mixing angle $\Theta = 92°$ suggests that OO is dominated by SE coupling in agreement with theoretical predictions.

We thank M. V. Eremin, T. Kopp, and K.-H. Höck for fruitful discussions. This work was supported by the BMBF under Contract No. 13N6917 (EKM) and partly by the DFG via the SFB 484 and DFG/RFFI-Project No. 436-RUS 113/566/0. B. I. K. and E. S. were partially supported by CRDF via Grant No. REC-007.

[1] Y. Tokura and N. Nagaosa, Science **288**, 462 (2000).
[2] H.A. Jahn and E. Teller, Proc. R. Soc. London **161**, 220 (1937).
[3] K.I. Kugel and D.I. Khomskii, Sov. Phys. Usp. **25**, 231 (1982).
[4] Y. Murakami, J.P. Hill, D. Gibbs, M. Blume, I. Koyama, M. Tanaka, H. Kawata, T. Arima, Y. Tokura, K. Hirota, and Y. Endoh, Phys. Rev. Lett. **81**, 582 (1998).
[5] Patrizia Benedetti, Jeroen van den Brink, Eva Pavarini, Assunta Vigliante, and Peter Wochner, Phys. Rev. B **63**, 060408 (2001).
[6] S. Ishihara and S. Maekawa, Rep. Prog. Phys. **65**, 561 (2002).
[7] J. Rodriguez-Carvajal, M. Hennion, F. Moussa, A.H. Moudden, L. Pinsard, and A. Revcolevschi, Phys. Rev. B **57**, R3189 (1998).
[8] J. Hemberger, H.-A. Krug von Nidda, V. Fritsch, J. Deisenhofer, S. Lobina, T. Rudolf, P. Lunkenheimer, F. Lichtenberg, A. Loidl, D. Bruns, and B. Büchner, Phys. Rev. Lett. **91**, 066403 (2003).
[9] M. Cwik, T. Lorenz, J. Baier, R. Müller, G. André, F. Bourée, F. Lichtenberg, A. Freimuth, R. Schmitz, E. Müller-Hartmann, and M. Braden, Phys. Rev. B **68**, 060401(R) (2003).
[10] G. Maris, Y. Ren, V. Volotchaev, C. Zobel, T. Lorenz, and T.T.M. Palstra, Phys. Rev. B **67**, 224423 (2003).
[11] J.B. Goodenough, Phys. Rev. **100**, 564 (1955).
[12] S. Okamoto, S. Ishihara, and S. Maekawa, Phys. Rev. B **65**, 144403 (2002).
[13] D.L. Huber, G. Alejandro, A. Caneiro, M.T. Causa, F. Prado, M. Tovar, and S.B. Oseroff, Phys. Rev. B **60**, 12 155 (1999).
[14] M. Tovar, G. Alejandro, A. Butera, A. Caneiro, M.T. Causa, F. Prado, and R.D. Sanchez, Phys. Rev. B **60**, 10 199 (1999).
[15] Joachim Deisenhofer, Michalis Paraskevopoulos, Hans-Albrecht Krug von Nidda, and Alois Loidl, Phys. Rev. B **66**, 054414 (2002).

[16] V.A. Ivanshin, J. Deisenhofer, H.-A. Krug von Nidda, A. Loidl, A.A. Mukhin, A.M. Balbashov, and M.V. Eremin, Phys. Rev. B **61**, 6213 (2000).
[17] G. Alejandro, C.A. Ramos, D. Vega, M.T. Causa, J. Fontcuberta, and M. Tovar, Physica B **320**, 26 (2002); (private communication).
[18] J. Deisenhofer, M.V. Eremin, D.V. Zakharov, V.A. Ivanshin, and R.M. Eremina, H.-A. Krug von Nidda, A.A. Mukhin, A.M. Balbashov, and A. Loidl, Phys. Rev. B **65**, 104440 (2002).
[19] H. Benner, M. Brodehl, H. Seitz, and J. Wiese, J. Phys. C **16**, 6011 (1983).
[20] M. Paraskevopoulos, F. Mayr, J. Hemberger, A. Loidl, R. Heichele, D. Maurer, V. Müller, A.A. Mukhin, and A.M. Balbashov, J. Phys.: Condens. Matter **12**, 3993 (2000).
[21] A. Pimenov, M. Biberacher, D. Ivannikov, A. Loidl, V.Yu. Ivanov, A.A. Mukhin, and A.M. Balbashov, Phys. Rev. B **62**, 5685 (2000).
[22] N.O. Moreno, P.G. Pagliuso, C. Rettori, J.S. Gardner, J.L. Sarrao, J.D. Thompson, D.L. Huber, J.F. Mitchell, J.J. Martinez, and S.B. Oseroff, Phys. Rev. B **63**, 174413 (2001).
[23] Q. Huang, A. Santoro, J.W. Lynn, R.W. Erwin, J.A. Borchers, J.L. Peng, and R.L. Greene, Phys. Rev. B **55**, 14 987 (1997).
[24] A. Abragam and B. Bleaney, *Electron Paramagnetic Resonance of Transition Ions* (Clarendon, Oxford, 1970).
[25] B.I. Kochelaev, E. Shilova, J. Deisenhofer, H.-A. Krug von Nidda, A. Loidl, A.A. Mukhin, and A. M Balbashov, Mod. Phys. Lett. B **17**, 459 (2003).
[26] M.C. Sánchez, G. Subías, J. García, and J. Blasco, Phys. Rev. Lett. **90**, 045503 (2003).
[27] Ryo Maezono, Sumio Ishihara, and Naoto Nagaosa, Phys. Rev. B **58**, 11 583 (1998).
[28] K. Tobe, T. Kimura, Y. Okimoto, and Y. Tokura, Phys. Rev. B **64**, 184421 (2001).
[29] O. Sikora and A. Oles, Acta Phys. Pol. B **34**, 861 (2003).